Apoptosis in severe, compensated pressure overload predominates in nonmyocytes and is related to the hypertrophy but not function

Ricardo J. Gelpi, Misun Park, Shumin Gao, Sunil Dhar, Dorothy E. Vatner and Stephen F. Vatner

Am J Physiol Heart Circ Physiol 300:H1062-H1068, 2011. First published 10 December 2010; doi:10.1152/ajpheart.00998.2010

Am J Physiol Heart Circ Physiol 300: H1062–H1068, 2011.
First published December 10, 2010; doi:10.1152/ajpheart.00998.2010.

Apoptosis in severe, compensated pressure overload predominates in nonmyocytes and is related to the hypertrophy but not function

Ricardo J. Gelpi,[1,2]* Misun Park,[1]* Shumin Gao,[1] Sunil Dhar,[1] Dorothy E. Vatner,[1] and Stephen F. Vatner[1]

[1]*Cardiovascular Research Institute and the Department of Cell Biology & Molecular Medicine, University of Medicine and Dentistry of New Jersey, New Jersey Medical School, Newark, New Jersey; and* [2]*Faculty of Medicine, Institute of Cardiovascular Physiopathology and the Department of Pathology, University of Buenos Aires, Buenos Aires, Argentina*

Submitted 4 October 2010; accepted in final form 9 December 2010

Gelpi RJ, Park M, Gao S, Dhar S, Vatner DE, Vatner SF. Apoptosis in severe, compensated pressure overload predominates in nonmyocytes and is related to the hypertrophy but not function. *Am J Physiol Heart Circ Physiol* 300: H1062–H1068, 2011. First published December 10, 2010; doi:10.1152/ajpheart.00998.2010.—It is widely held that myocyte apoptosis in left ventricular hypertrophy (LVH) contributes to left ventricle (LV) dysfunction and heart failure. The main goal of this investigation was to determine if there is a statistical relationship among LV hypertrophy, apoptosis and LV function, and importantly whether the apoptosis occurs in myocytes or nonmyocytes in the heart. We used both rat and canine models of severe LVH induced by chronic thoracic aortic banding with resultant LV-aortic pressure gradients 145–155 mmHg and increases in LV/body weight of 58 and 70%. These models also provided the ability to examine transmural apoptosis in LVH. In both models, the overwhelming majority (88%) of apoptotic cells were nonmyocytes. The regressions for apoptosis vs. LVH were stronger for nonmyocytes than myocytes and also stronger in the subendocardium than the subepicardium. Importantly, LV systolic and diastolic wall stresses were normal, indicating that the apoptosis could not be attributed to LV stretch or heart failure. In addition, there was no relationship between the extent of apoptosis and LV ejection fraction, which actually increased ($P < 0.05$), in the face of elevated LV systolic pressure, indicating that greater apoptosis did not result in a decrease in LV function. Thus, in response to chronic, severe pressure overload, LVH in the absence of LV dilation, and elevated LV wall stress, apoptosis occurred predominantly in nonmyocytes in the myocardial interstitium, more in the subendocardium than the subepicardium. The extent of apoptosis was linearly related to the amount of LV hypertrophy, but not to LV function.

heart failure; left ventricular hypertrophy; programmed cell death; left ventricular wall stress

IT IS WIDELY RECOGNIZED THAT apoptosis increases with left ventricular hypertrophy (LVH) and that the increased apoptosis is a critical mechanism mediating the transition from compensated hypertrophy to heart failure (1, 2, 4, 10, 12, 16). This concept is based on the tacit assumption that the apoptosis occurs in myocytes and that the reduction in contractile units in the heart leads to failure. However, 75% (by the cell number) of the cells in the heart are nonmyocytes (7). Interestingly, in models of heart failure, particularly those that involve injury to the heart, e.g., ischemia (8, 11, 14) or with pressure overload, LVH where LV wall stress is increased or LV decompensation has occurred (3, 5, 13) have shown that apoptosis also occurs in nonmyocytes in the heart. Whether nonmyocyte apoptosis occurs in the compensated hypertrophied heart without an increase in wall stress, particularly in the absence of myocardial infarction and injury, is not known. Furthermore, it is not known whether apoptosis relates to the severity of LVH, whether it results in reduced LV function with more severe LVH, and whether there is a transmural distribution of apoptosis.

The goal of this investigation was first to determine the relationship between the extent of LVH and apoptosis where LVH was induced by chronic thoracic aortic banding, and whether with more severe LVH, LV function begins to decline. The most important goal was to determine the extent to which the apoptosis occurred in myocytes or nonmyocytes. To answer these questions, it was important to study models of pure hypertrophy, where decompensation had not occurred, and myocytes were not stretched, since myocyte stretching also leads to apoptosis (6). In addition, in heart failure, many neurohormonal adjustments occur, which can also affect apoptosis (15, 18). Accordingly, we measured LV function and wall stress and verified that the hearts were well compensated, despite severe LVH. We employed models of chronic pressure overload LVH induced by aortic banding, both in dogs and rats. These models permitted evaluation of transmural apoptosis and were characterized by LV-aortic pressure gradients over 140 mmHg, levels not generally achieved in prior studies of thoracic aortic banding, yet LV wall stress and end-diastolic dimensions and pressures remained normal.

METHODS

Experimental Animal Models

Aortic banding in rats and measurement of LV function. Male Sprague-Dawley rats (2.7 ± 0.1 mo of age) were used for transverse aortic constriction (TAC) and sham-operation in accordance with the Institutional Animal Care and Use Committee (IACUC) at the New Jersey Medical School. These studies were reviewed and approved by the IACUC at the New Jersey Medical School. Rats were anesthetized with a mixture of ketamine and xylazine (60 and 6 mg/kg, respectively). The sternum was cut to the level of the second rib and retracted sidewise to expose the thymus and the aorta. TAC was created by tying a 6–0 braided polyester suture around the transverse aorta against a 21-gauge needle, which was then removed. Four weeks after aortic banding, closed-chest catheterization was performed. Two high-fidelity catheter tip transducers (1.4 Fr; Millar) were used; one was inserted in the right carotid artery and carefully advanced to the left ventricle (LV), and the other was placed in the left femoral artery and abdominal aorta. The pressures in the LV and abdominal aorta were measured simultaneously to calculate the pressure gradient.

* R. J. Gelpi and M. Park contributed equally to this work.

Address for reprint requests and other correspondence: S. F. Vatner, UMDNJ-New Jersey Medical School, Dept. of Cell Biology & Molecular Medicine, 185 South Orange Ave., MSB G-609, Newark, NJ 07103 (e-mail: vatnersf@umdnj.edu).

Transthoracic echocardiography was performed using an Acuson Sequoia 256 ultrasound system with a 13-MHz linear transducer. Echocardiography studies were performed under light anesthesia (Avertin, 2.5%-0.012 ml/g ip), the chest was shaved, and the animal was then placed on a warmed pad. Electrode needles were connected to each limb (Grass Technologies), and the electrocardiogram was simultaneously recorded. Mice were imaged in a shallow left lateral decubitis position. Two-dimensional parasternal short-axis imaging plane was used to obtain M-mode tracings at the level of the papillary muscles. LV internal dimensions and LV wall thickness were determined at systole and diastole. End-diastolic measurements were taken at the maximal LV diastolic dimension, and end systole was defined as the time of the most anterior systolic excursion of the posterior wall. Measurements were taken from three consecutive beats for each rat. Systolic function was evaluated from LV dimensions by the cubed method as percentage of LV ejection fraction (LVEF): LVEF (%) = $[(LVEDD^3 - LVESD^3)/LVEDD^3] \times 100$, where LVEDD and LVESD are LV end-diastolic diameter and LV end-systolic diameter. LV systolic wall stress (LVSWS) was calculated as: LVSWS (g/cm^2) = $(1.35 \times LVSP \times LVIDs)/[4 \times LVPWs \times (1 + LVPWs/LVIDs)]$, where LVSP stands for LV systolic pressure and LVIDs and LVPWs stand for LV internal diameter and LV posterior wall thickness in systole, respectively. The same calculation was performed for LV diastolic wall stress but considering the diastolic pressure and dimensions.

Aortic banding in dogs and LV function measurement. Mongrel dogs of either sex at 8–10 wk of age were anesthetized with 12.5 mg/kg sodium thiamylal maintained with halothane anesthesia (1–2 vol/100 vol) and ventilated with a respirator (Harvard apparatus). A right thoracotomy was performed through the fourth intercostal space by use of sterile surgical technique. The ascending aorta above the coronary arteries was isolated and dissected free of surrounding tissue. A 1-cm-wide Teflon cuff was placed around the aorta and tightened until a thrill could be palpated over the aortic arch. Next, the chest was closed. The Teflon band created a fixed supravalvular aortic lesion that became relatively more stenotic as the animals grew. The dogs were followed for 10–15 mo. After that, aortic-banded and sham dogs were instrumented. Tygon catheters were implanted in the descending thoracic aorta and left atria of all dogs. A solid-state miniature pressure transducer (model P22; Konigsberg Instruments) was implanted in the apex to measure LV pressure in banded dogs and in control dogs.

Also, piezoelectric ultrasonic dimension crystals were implanted on opposing anterior and posterior subendocardial surfaces of the LV to measure the short-axis internal diameter and on opposing subendocardial and subepicardial surfaces in the same equatorial plane as the internal diameter crystals to measure wall thickness. Pacing electrodes were sutured to the left atrial appendage. The thoracotomy incision was closed in layers, and the animals were allowed to recover for 2–4 wk before study.

Detection of Apoptosis

Tissue samples of LV from rat and dog were fixed by immersion in 10% neutralized buffered formalin and embedded in paraffin. After 5-μm-thick serial sectioning of heart paraffin block, DNA fragmentation was detected in situ by using the terminal deoxyribonucleotide transferase (TdT)-mediated dUTP nick-end labeling (TUNEL) kit (Roche) according to the manufacturer's instructions. Briefly, the paraffin sections were deparaffinized by immersing in xylene; rehydrated through 100, 95, 70, and 0% ethanol; after incubation with proteinase K (20 μg/ml) (Sigma-Aldrich), the sections were washed in PBS. DNA fragments in the sections were labeled with 2 nmol/l biotin-conjugated dUTP and 0.1 U/μl TdT for 30 min at 37°C. The incorporation of biotin-16-dUTP in DNA was determined by incubating the sections with streptavidin, Alexa Fluor-488 conjugated (1:500; Invitrogen). To discriminate apoptosis in nonmyocytes and myocytes, tissue sections were counterstained with rhodamine-conjugated wheat germ agglutinin (WGA) (DAPI; Vector Laboratories) described as in our previous study (13). WGA stains all cell membranes in LV myocytes. The pattern of WGA staining is seen not only at the outer membrane but also followed a striated pattern in myocytes (Fig. 2). Sections were mounted using Vectashield mounting medium containing 4,6-diamidino-2-phenylindole (Vector Laboratories).

TUNEL-positive cells were counted separately in subendocardium and subepicardium of the LV from reading of 106 ± 3 fields (10.6 mm^2) in each area at ×60 magnification using an Olympus BX51 Fluorescence Microscope. Total TUNEL-positive cell numbers were determined by the average from three different sections of each animal. Nuclei/field were calculated from nuclei counting of 20 fields from each animal using the same magnification. Apoptotic rate was expressed as the percentage of TUNEL-positive cells per nuclei.

Immunohistochemical Staining

For characterization of cell types of apoptotic nonmyocytes, 5-μm serial tissue sections were immunostained with the following antibodies: mouse anti-rat CD68 (1:50 dilution; AbD Serotec) for macrophages; mouse monoclonal anti-heat shock protein (HSP) 47 (1:100 dilution; Stressgen) for fibroblasts; and isolectin GS-IB_4 from *Griffonia simplicifolia*, Alexa Fluor-568 conjugated (1:50 dilution; Invitrogen) for endothelial cells. Antigen retrieval was performed by immersing sections in 10 mM citrate buffer (pH 6.0) and boiling under pressure for 10–20 min. The tissue sections were incubated with the blocking solution (Protein Block Serum-Free; DAKO) for 15 min at room temperature. Sections were incubated with primary antibody at 4°C for overnight, washed in PBS, and then incubated later with goat anti-mouse Alexa Fluor-555-conjugated (Invitrogen) secondary antibody. Apoptotic nonmyocytes were detected by dual staining with TUNEL assay.

Statistics

Data reported are means ± SE. Student's *t*-tests were used to compare sham with 4 wk TAC with a significance level of $P < 0.05$. Simple regressions were conducted with LV/body weight as the dependent variable and apoptosis as the independent variable. Wherever subendocardium was being compared with subepicardium, the paired *t*-tests were applied to compare their means at the $P < 0.05$ significance level.

RESULTS

The extent of LVH and the hemodynamics are shown in Table 1 (rat) and Table 2 (dog). The LV/aortic pressure gradients were similar in rats (151 ± 7 mmHg) and dogs (143 ± 17 mmHg). The amount of LVH, i.e., the LV/body weight, in-

Table 1. *Rat physiological parameters*

	Sham (n = 8)	TAC (n = 11)
LV/BW	2 ± 0.1	3 ± 0.1*
Lung/BW	3 ± 0.1	4 ± 0.1
LV EF, %	73 ± 1.3	78 ± 1.8*
LV FS, %	35 ± 1.0	40 ± 1.7*
Heart rate, beats/min	290 ± 13	299 ± 5.0
LVEDP, mmHg	5 ± 0.9	5 ± 1.0
LV +dP/dt, mmHg/s	6,825 ± 180	8,273 ± 273*
LV -dP/dt, mmHg/s	5,638 ± 229	9,045 ± 426*
LV systolic wall stress, g/cm^2	60 ± 3.1	68 ± 7.6
LV diastolic wall stress, g/cm^2	8 ± 1.5	5 ± 1.1*
LV-aortic pressure gradient, mmHg		151 ± 6.6

Values are means ± SE; n, no. of rats. TAC, transverse aortic constriction; LV, left ventricle; BW, body weight; EF, ejection fraction; FS, fractional shortening; LVEDP, LV end-diastolic pressure. *$P < 0.05$.

Table 2. *Dog physiological parameters*

	Sham (n = 4)	TAC (n = 5)
LV/BW	4 ± 0.3	7 ± 0.6*
LV FS, %	23 ± 2.3	21 ± 3.8
Heart rate, beats/min	87 ± 3.0	91 ± 6.0
LVEDP, mmHg	9 ± 1.2	12 ± 2.1
LV +dP/dt, mmHg/s	3,179 ± 151	3,379 ± 121
LV -dP/dt, mmHg/s	2,927 ± 190	3,978 ± 326
LV systolic wall stress, g/cm^2	204 ± 17	249 ± 26
LV diastolic wall stress, g/cm^2	22 ± 2.0	17 ± 1.0
LV-aortic pressure gradients, mmHg		143 ± 17

Values are means ± SE; n, no. of dogs. *$P < 0.05$.

creased similarly in rats 58% and dogs 70%. LV wall stress was normalized by LVH, and LV end-diastolic pressure was not elevated in LVH. Lung/body weight, an index of heart failure, was not elevated with LVH in rats (Table 1). LV function did not decline in the dog model and actually increased ($P < 0.05$) in the rat model. For example, in rats, LV fractional shortening was elevated in LVH (40 ± 1.7%) compared with sham (35 ± 1.0%), and both positive and negative LV dP/dt were significantly increased (Table 1).

In Figs. 1–6, the amount of apoptosis was evaluated for total apoptotic cells (both myocytes and nonmyocytes combined) as well as for only myocytes and only nonmyocytes. In Figs. 1–6, the data are presented for both the subendocardium and the subepicardium. The amount of apoptosis tended to be greater, but not significantly, in the subendocardium compared with subepicardium for total cells and for nonmyocytes. Data were similar in dogs with LVH. The bar graphs in Fig. 1 show the apoptosis data from rats (Fig. 1*A*) and dogs (Fig. 1*B*). In the rat model, the percentage of apoptotic cells for nonmyocytes was five- to sevenfold greater (0.12 ± 0.01, $P < 0.05$) than for myocytes (0.02 ± 0.00), and this was observed both in the subendocardium and subepicardium. The detection of apoptosis was performed by double staining with TUNEL and WGA for discriminating apoptotic myocytes and nonmyocytes (Fig. 2*A*). The representative photographs of apoptotic myocytes and apoptotic nonmyocytes are shown in Fig. 2, *B* and *C*.

To characterize the cell types of TUNEL-positive nonmyocytes, the rat myocardial sections were stained with antibodies

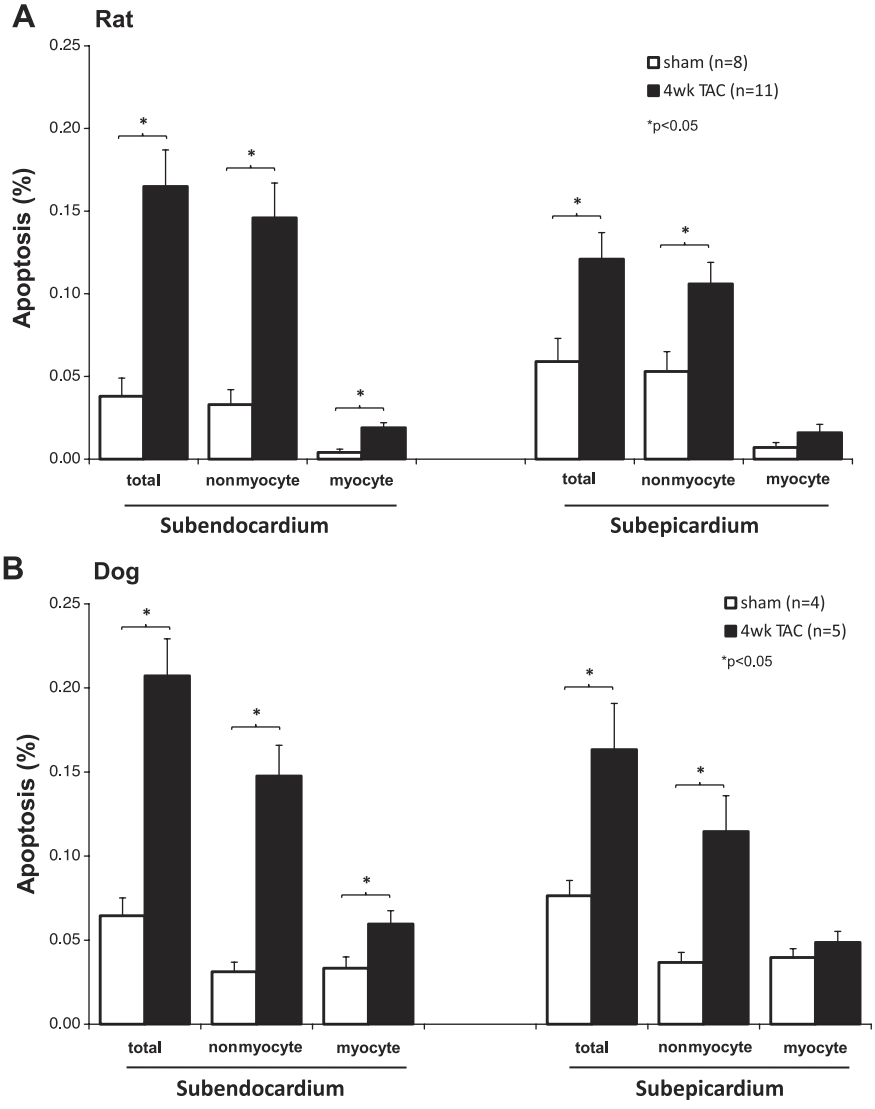

Fig. 1. *A*: apoptosis in rat model of transverse aortic constriction (TAC). This figure compares the apoptosis (%) in left ventricular hypertrophy (LVH) after 4 wk of TAC (filled bars) vs. sham-operated rats (open bars) in the subendocardium (*left*) and subepicardium (*right*) for myocytes and for nonmyocytes. Apoptosis increased significantly more in LVH for both nonmyocytes and myocytes subendocardially (*left*) and for nonmyocytes subepicardially (*right*). *B*: dog model of TAC. The data resembled those from the rat model. Apoptosis is compared in 4 wk TAC with sham (*$P < 0.05$).

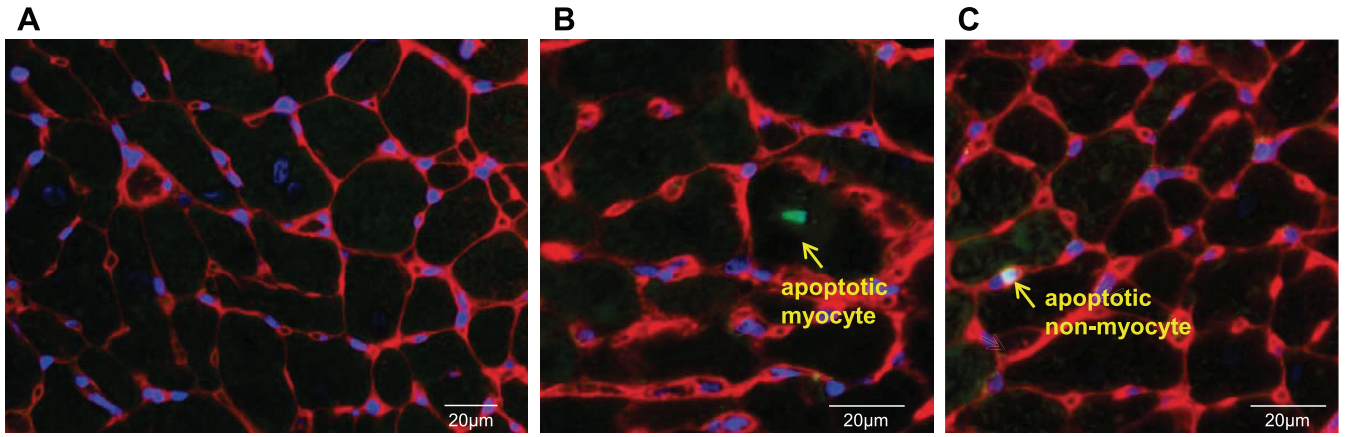

Fig. 2. Apoptosis of the myocardium in rat with LVH. *A*: representative photograph of wheat germ agglutinin (WGA) staining using ×60 magnification. The outlines of myocytes are shown by WGA staining (red), and nuclei are stained with 4,6-diamidino-2-phenylindole (DAPI, blue). *B* and *C*: representative photograph of apoptotic myocyte and apoptotic nonmyocyte by double staining with terminal deoxyribonucleotide transferase-mediated dUTP nick-end labeling (TUNEL) and WGA. Arrows signify a TUNEL-positive myocyte (green, *middle*) and TUNEL-positive nonmyocyte (green, *right*) from a rat with LVH. Scale bar: 20 μm.

recognizing macrophages (CD68), endothelial cells (isolectin GS-IB_4), and fibroblasts (HSP47). Representative images of apoptotic nonmyocytes in LVH are shown in Fig. 3.

The regression relationships between the amount of apoptosis and the amount of hypertrophy are shown for total cells (Fig. 4), nonmyocytes (Fig. 5), and myocytes (Fig. 6). The R^2 and P values for the regressions are shown in Figs. 4–6. There were significant linear relationships between the amount of apoptosis and the amount of hypertrophy in the subendocardium for total cells and for nonmyocytes. However, the corresponding relationships were weaker in the subepicardium as reflected by the R^2 value and were not significant for myocytes, most likely because the amount of apoptosis in myocytes was relatively trivial. There was virtually no relationship between

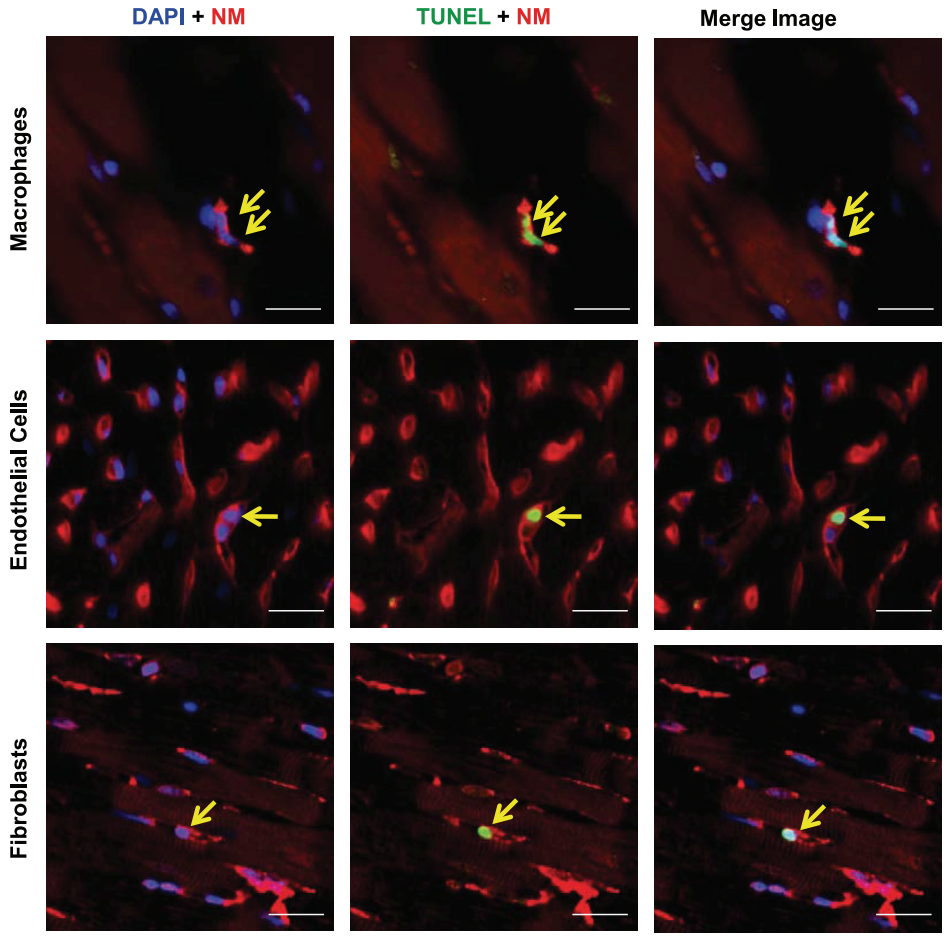

Fig. 3. Characterization of cell types for apoptotic nonmyocytes in rat LVH. Representative photographs of apoptotic nonmyocytes (arrows) by double staining with TUNEL and specific antibodies (CD68 for macrophages, isolectin GS-IB4 for endothelial cells, and HSP47 for fibroblasts) using ×60 magnification. *Left*: nonmyocyte with DAPI. *Middle*: TUNEL-positive nonmyocyte. *Right*: the merged image of an apoptotic nonmyocyte. Green: TUNEL; red: nonmyocytes (NM); blue: DAPI. Scale bar: 20 μm.

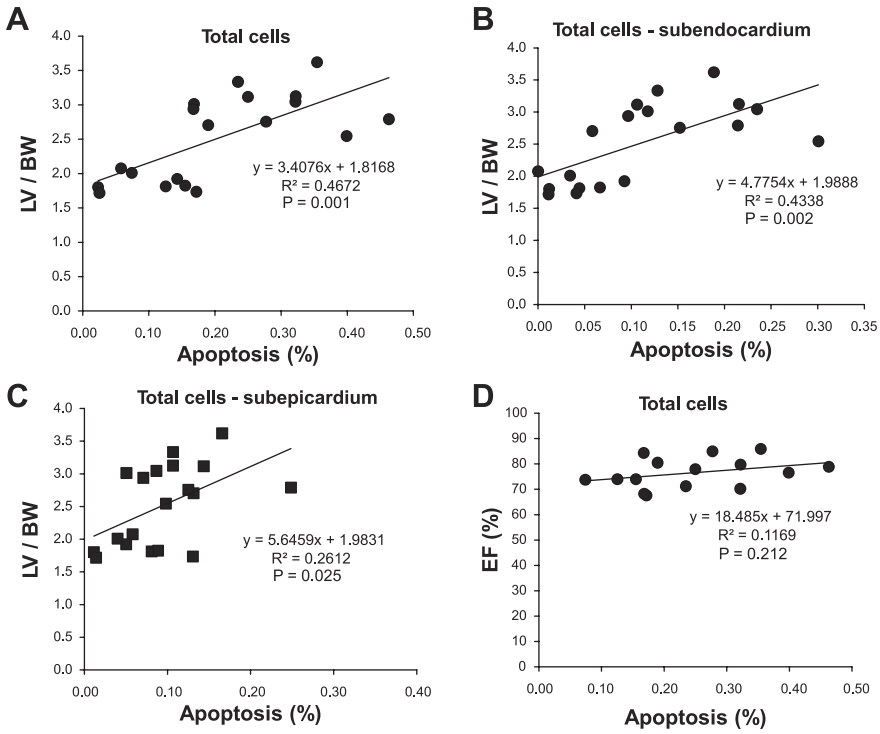

Fig. 4. Rat model of TAC. The relationship between apoptosis and the left ventricle (LV)/body wt (BW) is shown for total cells (*A*), in subendocardium (*B*), and in subepicardium (*C*). All of these correlations were very significant (R^2 and *P* values for regressions are shown). In contrast, there was no significant relationship between the amount of apoptosis and LV ejection fraction (EF, %) (*D*), i.e., LV EF (%) did not decline with increasing amounts of apoptosis with chronic severe LVH.

the amount of apoptosis and LV function, i.e., LV ejection fraction for all the groups (Figs. 4–6).

DISCUSSION

The major finding of the present investigation was that apoptosis in the severe but well-compensated hypertrophied heart occurs not in myocytes, as previously thought, but rather predominantly in interstitial nonmyocytes and that it is related to the extent of LVH. Nonmyocyte apoptosis has been noted before in models of heart failure, particularly those that involve injury to the heart, e.g., ischemia (8, 12, 15) or with pressure overload LVH where LV wall stress is increased or LV decompensation has occurred (3, 5, 13). However, almost all studies of apoptosis and LVH have concluded that the apoptosis affected myocytes (1, 2, 4, 10, 12, 13, 16). Furthermore, most of these studies did not document that the LVH was

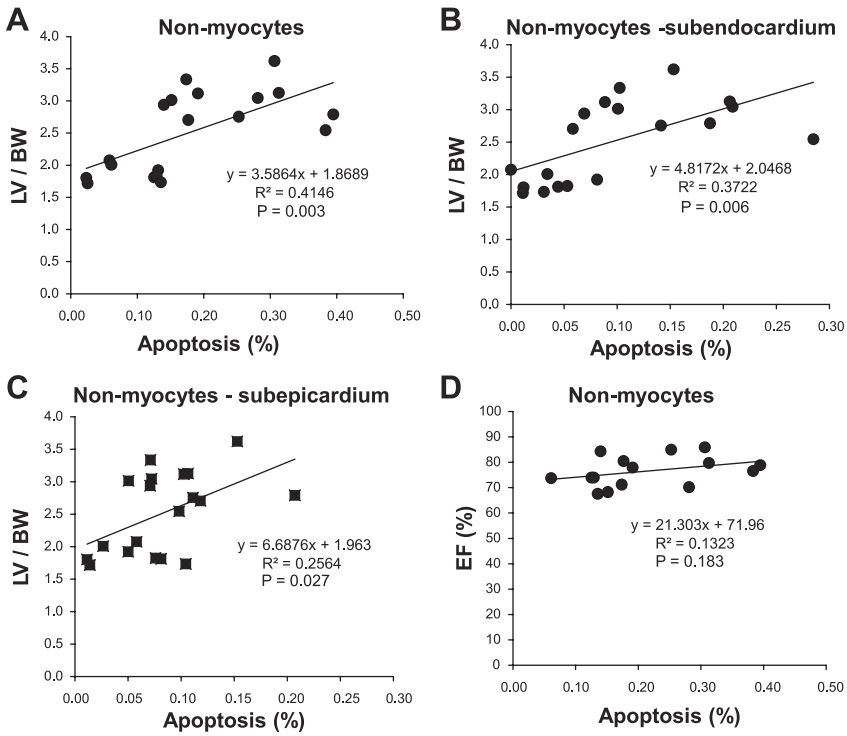

Fig. 5. Rat model of TAC. The relationship between apoptosis and LV/BW is shown for nonmyocytes (*A*), in subendocardium (*B*), and in subepicardium (*C*). All of these correlations were very significant (R^2 and *P* values for regressions are shown). The correlations were stronger in subendocardium than subepicardium. In contrast, there was no significant relationship between the amount of apoptosis and LV EF (%) (*D*), i.e., LV EF (%) did not decline with increasing amounts of nonmyocyte apoptosis in subendocardium with chronic severe LVH.

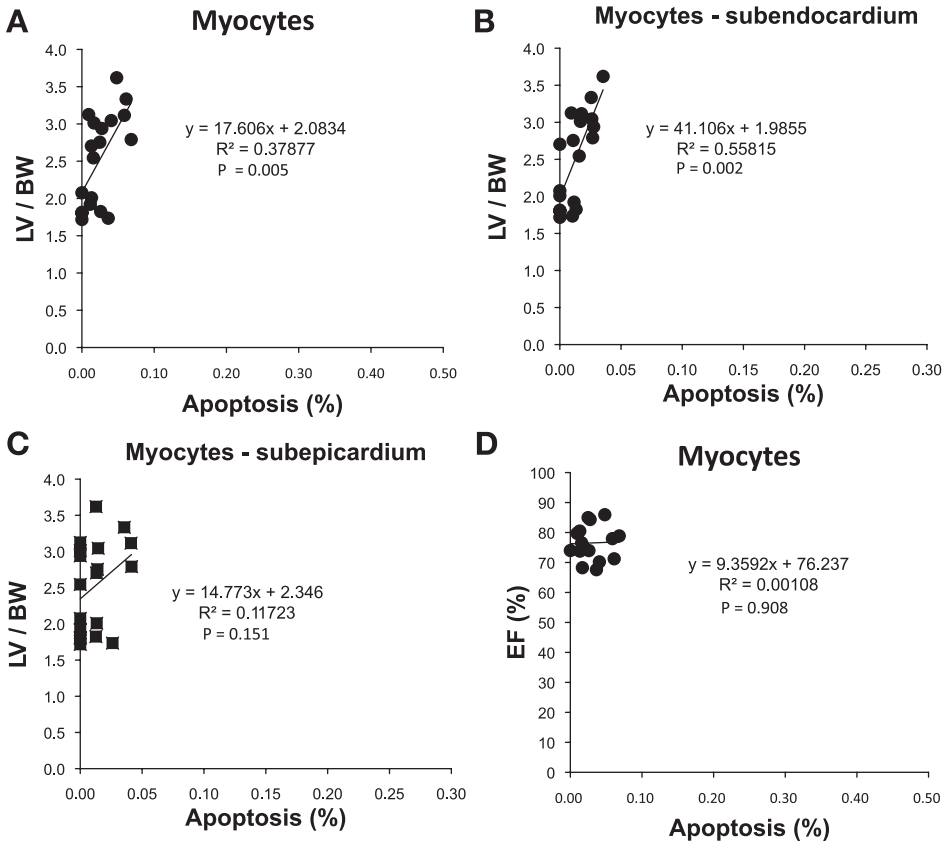

Fig. 6. Rat model of TAC. The relationship between apoptosis and LV/BW is shown for myocytes (*A*), in subendocardium (*B*), and in subepicardium (*C*). The correlations for transmural apoptosis and subendocardium apoptosis were very significant (R^2 and P values for regressions are shown). In contrast, the correlation was weak in the subepicardium, and there was still no significant relationship between the amount of apoptosis and LV EF (%) (*D*), i.e., LV EF (%) did not decline with increasing amounts of myocyte apoptosis with chronic severe LVH.

compensated and wall stress was normalized. This is an important point since apoptosis is known to be increased with myocardial dilatation and in heart failure (1, 5, 9, 14, 15). In the current investigation, both in the rat and the dog model of chronic pressure overload induced by thoracic aortic banding, the pressure gradients from LV to aorta were higher (145–155 mmHg) than most other previous studies, but the hearts were well compensated, i.e., LV end-diastolic pressure was not elevated and LV systolic and diastolic wall stresses were normal. Surprisingly, LV function was enhanced, as reflected by significantly increased LV fractional shortening in the face of markedly elevated LV systolic pressure along with increased LV d*P*/d*t*.

LVH and cardiac remodeling contribute to the development and progression of heart failure. However, the mechanisms that contribute to the structural changes that underlie progressive cardiac remodeling are only partially understood. Although it is generally held that LVH results in enhanced apoptosis of myocytes and that the loss of these myocytes is an important mechanism leading to decompensation of the hypertrophied heart, resulting in heart failure (1, 2, 4, 10, 12, 16), our data do not support this concept for two reasons. First, the amount of myocyte apoptosis was relatively trivial such that there would be an insignificant amount of loss of myocardial mass. Second, there was no relationship between the amount of apoptosis and LV function, i.e., LV ejection fraction. If increased apoptosis was the cause of reduced LV function, then there should have been at least a trend toward reduced function in those hearts that showed the most apoptosis. However, this was not observed, indicating, as a minimum, that the amount of apoptosis that occurred in this study with severe LVH was not sufficient to affect cardiac function adversely. Because the overwhelming majority of apoptotic cells were in nonmyocytes, it is not surprising that LV function was not compromised by the apoptosis. These data are also consistent with the results from a prior study from our laboratory in a monkey model of myocardial infarction and heart failure (14). Although the amount of apoptosis increased when heart failure developed in that study (14), the apoptosis still occurred predominantly in nonmyocytes.

An elegant study by Wencker et al. (17), using a transgenic model to induce myocyte apoptosis, found that amounts of myocyte apoptosis similar to what was observed in the current study led to LV dysfunction, heart failure, and dilation (17). If the amount of apoptosis is similar in the two studies, it raises the questions why did LV function decrease in the transgenic model? Or conversely, why did LV function improve in the current model of chronic pressure overload used in the current investigation? The differences in the two studies are not easily reconciled. One difference is the use of a physiological intervention, chronic pressure overload in an otherwise normal animal vs. a transgenic model that may affect other genes and signaling pathways. In support of the possibility that the transgenic model is affected by more than apoptosis, it would be important to know if LV weight was significantly less in the transgenic model due to a loss of myocytes before heart failure developed, since the underlying concept is that myocyte apoptosis leads to reduced contractile elements in the heart thereby compromising LV contraction; however, these data are not available (17). Conversely, if the LV mass does not decrease

due to the excessive myocyte apoptosis, then how does the heart fail? Second, in our study, we demonstrated the importance of nonmyocyte apoptosis, which conceivably could be salutary and offset the adverse effects of myocyte apoptosis. One other consideration that needs to be examined in both models is whether apoptosis is a physiological, not a pathological, process whereby damaged myocytes are replaced by myocyte regeneration, which could offset the effects of apoptosis. Taking all these considerations together, we believe our study challenges the concept that myocyte apoptosis is a major mechanism leading to heart failure in the setting of chronic pressure overload LVH. Certainly, in the confines of the current protocol, there was no evidence that myocyte apoptosis, which increased linearly with LVH, had any adverse effect on LV function. However, more studies will have to be done in the future to determine the extent to which myocyte apoptosis is detrimental or the nonmyocyte apoptosis is salutary, particularly extending the model to LV decompensation.

There were two other findings of the present study that have not been appreciated previously. The first is that there was a significant relationship between the amount of apoptosis and the amount of hypertrophy. Although this might be predicted from prior studies demonstrating increased apoptosis with LVH, it has not been shown clearly previously. The second new finding is that we examined apoptosis in the subendocardium and the subepicardium. It might be predicted that the apoptosis would be more severe subendocardially, since that part of the hypertrophied heart is more susceptible to ischemia. We found that the relationships between the amount of apoptosis and the amount of LVH were stronger in the subendocardium for both myocytes and nonmyocytes, but the amount of apoptosis was not significantly greater in the subendocardium. A previous study found that there was more apoptosis subendocardially, when the hypertrophied heart began to fail, but not in well-compensated LVH (4).

In summary, these data indicate that myocyte apoptosis is relatively minor in response to pressure overload LVH in the absence of LV dilation and elevated LV wall stress, but rather the increased apoptosis predominantly occurs in nonmyocytes in the myocardial interstitium, which is linearly related to the amount of LVH. In contrast, there was no significant relationship between the amounts of apoptosis of LV systolic function, which actually increased in the rat model of severe hypertrophy. These results suggest that mechanisms other than apoptosis may be more important in mediating the transition to heart failure in the hypertrophied heart.

GRANTS

This study was supported, in part, by NIH Grants HL-069020, H-L101420, HL-033107, HL-093481, HL-102472, HL-069752, AG-027211, and HL-095888.

DISCLOSURES

No conflicts of interest are declared by the authors.

REFERENCES

1. **Anselmi A, Gaudino M, Baldi A, Vetrovec GW, Bussani R, Possati G, Abbate A.** Role of apoptosis in pressure-overload cardiomyopathy. *J Cardiovasc Med (Hagerstown)* 9: 227–232, 2008.
2. **Choi YH, Cowan DB, Moran AM, Colan SD, Stamm C, Takeuchi K, Friehs I, del Nido PJ, McGowan FX Jr.** Myocyte apoptosis occurs early during the development of pressure-overload hypertrophy in infant myocardium. *J Thorac Cardiovasc Surg* 137: 1356–1362, 2009.
3. **Condorelli G, Morisco C, Stassi G, Notte A, Farina F, Sgaramella G, de Rienzo A, Roncarati R, Trimarco B, Lembo G.** Increased cardiomyocyte apoptosis and changes in proapoptotic and antiapoptotic genes bax and bcl-2 during left ventricular adaptations to chronic pressure overload in the rat. *Circulation* 99: 3071–3078, 1999.
4. **Engel D, Peshock R, Armstong RC, Sivasubramanian N, Mann DL.** Cardiac myocyte apoptosis provokes adverse cardiac remodeling in transgenic mice with targeted TNF overexpression. *Am J Physiol Heart Circ Physiol* 287: H1303–H1311, 2004.
5. **Ikeda S, Hamada M, Hiwada K.** Contribution of non-cardiomyocyte apoptosis to cardiac remodeling that occurs in the transition from compensated hypertrophy to heart failure in spontaneously hypertensive rats. *Clin Sci (Lond)* 97: 239–246, 1999.
6. **Jiang L, Huang Y, Hunyor S, dos Remedios CG.** Cardiomyocyte apoptosis is associated with increased wall stress in chronic failing left ventricle. *Eur Heart J* 24: 742–751, 2003.
7. **Jugdutt BI.** Ventricular remodeling after infarction and the extracellular collagen matrix: when is enough enough? *Circulation* 108: 1395–1403, 2003.
8. **Kanamori H, Takemura G, Li Y, Okada H, Maruyama R, Aoyama T, Miyata S, Esaki M, Ogino A, Nakagawa M, Ushikoshi H, Kawasaki M, Minatoguchi S, Fujiwara H.** Inhibition of Fas-associated apoptosis in granulation tissue cells accompanies attenuation of postinfarction left ventricular remodeling by olmesartan. *Am J Physiol Heart Circ Physiol* 292: H2184–H2194, 2007.
9. **Leri A, Barlucchi L, Limana F, Deptala A, Darzynkiewicz Z, Hintze TH, Kajstura J, Nadal-Ginard B, Anversa P.** Telomerase expression and activity are coupled with myocyte proliferation and preservation of telomeric length in the failing heart. *Proc Natl Acad Sci USA* 98: 8626–8631, 2001.
10. **Li XM, Ma YT, Yang YN, Liu F, Chen BD, Han W, Zhang JF, Gao XM.** Downregulation of survival signaling pathways and increased apoptosis in the transition of pressure overload-induced cardiac hypertrophy to heart failure. *Clin Exp Pharmacol Physiol* 36: 1054–1061, 2009.
11. **Li Y, Takemura G, Okada H, Miyata S, Kanamori H, Maruyama R, Esaki M, Li L, Ogino A, Ohno T, Kondo T, Nakagawa M, Minatoguchi S, Fujiwara T, Fujiwara H.** ANG II type 1A receptor signaling causes unfavorable scar dynamics in the postinfarct heart. *Am J Physiol Heart Circ Physiol* 292: H946–H953, 2007.
12. **Moorjani N, Ahmad M, Catarino P, Brittin R, Trabzuni D, Al-Mohanna F, Narula N, Narula J, Westaby S.** Activation of apoptotic caspase cascade during the transition to pressure overload-induced heart failure. *J Am Coll Cardiol* 48: 1451–1458, 2006.
13. **Muller P, Kazakov A, Semenov A, Bohm M, Laufs U.** Pressure-induced cardiac overload induces upregulation of endothelial and myocardial progenitor cells. *Cardiovasc Res* 77: 151–159, 2008.
14. **Park M, Shen YT, Gaussin V, Heyndrickx GR, Bartunek J, Resuello RR, Natividad FF, Kitsis RN, Vatner DE, Vatner SF.** Apoptosis predominates in nonmyocytes in heart failure. *Am J Physiol Heart Circ Physiol* 297: H785–H791, 2009.
15. **Ruffolo RR Jr, Feuerstein GZ.** Neurohormonal activation, oxygen free radicals, and apoptosis in the pathogenesis of congestive heart failure. *J Cardiovasc Pharmacol* 32, *Suppl* 1: S22–S30, 1998.
16. **Sharma AK, Dhingra S, Khaper N, Singal PK.** Activation of apoptotic processes during transition from hypertrophy to heart failure in guinea pigs. *Am J Physiol Heart Circ Physiol* 293: H1384–H1390, 2007.
17. **Wencker D, Chandra M, Nguyen K, Miao W, Garantziotis S, Factor SM, Shirani J, Armstrong RC, Kitsis RN.** A mechanistic role for cardiac myocyte apoptosis in heart failure. *J Clin Invest* 111: 1497–1504, 2003.
18. **Zhao J, Li J, Li W, Li Y, Shan H, Gong Y, Yang B.** Effects of spironolactone on atrial structural remodeling in a canine model of atrial fibrillation produced by prolonged atrial pacing. *Br J Pharmacol* 159: 1584–1594, 2010.